IEEE Robotics and Automation Letters (RA-L) paper, presented at ICRA 2023, London, UK. Cite as RA-L paper.

Development of a Novel 2-Dimensional Neck Haptic Device for Gait Balance Training

Hosu Lee†1, Amre Eizad†1, Jiho Park[1], Yeongmi Kim[2], Sunwoo Hwang[3], Min-Kyun Oh*4 and Jungwon Yoon*1, *Member, IEEE*

***Abstract*— Balance problems can be a major cause of falling. Existing gait balance rehabilitation devices usually have limited overground usability due to low portability. Therefore, there is need for development of a portable gait balance rehabilitation system. To fulfill this need, a wearable balance biofeedback system is proposed that utilizes a pair of novel devices to deliver 2-dimensional hybrid haptic biofeedback to the neck that is a combination of indentation and stretching of the skin corresponding to the mediolateral (ML) and anteroposterior (AP) directions, respectively. The system's functionality is demonstrated through an experiment where 14 healthy subjects and 1 stroke patient performed stance and gait tasks under various feedback conditions. Provision of feedback to healthy subjects resulted in significant improvements in two-dimensional balance under all task conditions. It is also observed that provision of feedback during more difficult tasks resulted in more significant balance improvements. Furthermore, use of the system during gait balance evaluation trials did not cause any significant change in gait speed, meaning that it does not have any detrimental effect on the user's gait. Results of the stroke subject pilot trial showed similar trends. We expect that use of the proposed system may help to improve the overground gait balance of people suffering from the after effects of diseases such as stroke.**

***Index Terms*— Haptics and Haptic Interfaces, Rehabilitation robotics, Wearable robotics.**

I. INTRODUCTION

The proportion of aging population is increasing globally, which is accompanied by an increase in the incidence of stroke [1]. Stroke survivors usually suffer from hemiplegia and sensory impairments that decrease their balancing ability, thus increasing their risk of falling [2]. Falling during gait not only causes physical injury, but also increases the fear of falling, which in turn further increases the risk of falling [3].

Balance training can increase gait stability and reduce risk of falling [4]. Recent researches have reported promising gait improvements through gait balance training for chronic stroke survivors [5]. However, the systems used for such trainings are usually cumbersome and may require interface with the user through sensory channels such as vision or hearing that are needed for environmental perception during free gait [5-7]. These factors reduce the usability of such systems for overground gait training in closer to real life environments.

Patients requiring gait balance rehabilitation can benefit from non-supportive kinesthetic contact with appropriately engineered structures such as instrumented canes, railings, etc. [8, 9]. However, these systems mostly require the patient to use their arm or hand to maintain continuous kinesthetic contact. In addition, due to their specific functional requirements, use of such systems is usually limited to lab or therapy clinic settings (fixed systems), or environments with smooth and hard floors (canes). A wearable feedback interface can allow the user to perform unrestricted over-ground gait. Wearable vibrotactile feedback systems have shown promising results in balance training applications [10]. However, vibration does not inherently include directional information, which limits its use in multi-dimensional balance applications such as combined provision of mediolateral (ML) and anteroposterior (AP) trunk tilts feedback. Recently, we developed a reaction wheel based wearable device to provide kinesthetic feedback of ML trunk tilts for balance improvement. The device improved balance during standing. However, due to low perception during gait and low feedback generation frequency, it could not be used for gait balance improvement [11, 12]. Another recently developed system utilizes a gyroscopic wheel to improve walking balance [13]. However, this system is excessively large and heavy, which limits its usability for people with gait impairments, such as stroke patients. Hence, there is need for a lightweight and easily wearable kinesthetic feedback device to generate multi-dimensional balance biofeedback that is compatible to use in the overground gait scenario.

Previously developed, directional haptic devices have been designed for application to the user's fingers or forearm [14-16]. Such area of application may cause hindrance to the hands during gait related movements and limit their usability during gait. Furthermore, the arms and hands can be rotated in large ranges of motion during walking and other activities of daily life. This rotation changes the alignments of their axes with those of the body, which can cause a directional feedback applied to the arm to lose meaning or provide misleading information. On the other hand, the neck has very small

Manuscript received: November 10, 2021; Accepted January 2, 2022.

This paper was recommended for publication by Editor Pietro Valdastri upon evaluation of the Associate Editor and Reviewers' comments. This work was supported by the National Research Foundation (NRF) of Korea (2019M3C1B809079812K) and by the GIST Research Institute (GRI) grant funded by GIST in 2021 *(*Corresponding authors: J. Yoon and M.K. Oh)*.

†Hosu Lee and Amre Eizad contributed equally to this work.

[1]H. Lee, A. Eizad, J. Park and J. Yoon are with School of Integrated Technology, Gwangju Institute of Science and Technology, South Korea. (e-mail: eldoon@nate.com; amre.eizad@gist.ac.kr; jiho-park@gist.ac.kr; jyoon@gist.ac.kr).

[2]Y. Kim is with Department of Mechatronics, MCI, Austria (e-mail: yeongmi.kim@mci.edu).

[3]S. Hwang is with Department of Rehabilitation Medicine, Gyeongsang National University School of Medicine, Gyeongsang National University Hospital, South Korea (e-mail: sunuhmed@naver.com).

[4]M. K. Oh is with Department of Rehabilitation Medicine, Gyeongsang National University School of Medicine, Gyeongsang National University Changwon Hospital, South Korea (e-mail: solioh21@hanmail.net).

Digital Object Identifier (DOI) : see top of this page.

movement relative to the perceived direction of the body, which makes it a suitable area for the application of directed cues. Additionally, it will free up the hands to move naturally during walking or to perform tasks related to daily life [12]

V. Krishnamoorthy et al. used an artificial finger attached to a static platform for light-touch interface with the neck and reported it had a greater effect on postural sway than interface with the fingertip [17]. In their arrangement, the fingertip indented the skin (normal pushing movement) when the body moved in ML direction and stretched it (tangential movement) when the body moved in AP direction. Taking inspiration from this, we have developed a novel 2-dimensional device to provide hybrid haptic feedback at the user's neck, which we have called the neck haptic device (NHD). The NHD provides feedback of ML trunk tilts in the form of normal skin indentation and of AP trunk tilts in the form of a stretch tangential to the skin surface. Human skin mechanical response modelling is very complex and highly dependent on a number of characteristics [18], and measurement of interaction forces between the skin and an external device is also a complex task [19]. Therefore, we have used mechanical deformation as the feedback modality in our developed device. This selection makes the device hardware and software design simple, which will enable us to translate its design into a widely usable and cost-effective rehabilitation system in the future. Using a pair of NHDs, placed one on each side of the user's neck, we have developed a wearable system that measures the trunk tilt of the user and provides balance corrective feedback to their neck. Furthermore, to verify the system's functionality, we have carried out stance and gait balance evaluations with 14 healthy and 1 stroke subject.

II. Development Of The System

A. System Design

The proposed system utilizes a pair of NHDs to provide feedback to the user about their ML and AP trunk tilts measured using the body worn sensor included in the system. Previous work showing the benefit of light touch to the neck during standing utilized 1N force [17]. However, due to the high amount of disturbance generated during walking, we assume that a higher magnitude force is required to ensure feedback perception. Additionally, a certain amount of normal force is required to ensure proper skin stretching. Therefore, to meet practical operational requirements and to ensure usability of the developed system for different studies in the future, we selected the maximum force output of 10N. Another work reported that, under controlled conditions, people are able to discern skin indentations and tangential deformations of minimum 1.5*mm* [20]. The neck has a high amount of soft tissue that can deform greatly due to the application of force. Therefore, to ensure usability of the system for a wide variety of subjects, the displacement requirement was set as 10*mm*. During quiet standing, highest reported COP (Center of pressure) movement frequency is 0.4Hz [21] and stepping frequency during 1.4*m/s* normal gait is reported to be 2Hz [22]. Therefore, the maximum cue generation frequency requirement of the system is set as 5Hz, which is more than double the reported stepping frequency.

Fig. 1 shows the 3D model of the right side NHD. The left side NHD is similar in design with the only difference being a reversed base structure. This base structure, which is aligned to the AP direction of the body, allows the device to be moved diagonally over a range of ±40*mm* to allow combined adjustment in the vertical and AP directions (Fig. 1 (a)). The device is setup as a RP (Revolute and Prismatic) serial manipulator. The base of the rotary actuator is fixed to a plate that is hinged to the base structure. The angle of this plate can be adjusted between 0 and 25 degrees in 5 degree increments by inserting angle adjustment blocks between the structural components, as shown in Fig. 1 (a). The linear actuator is attached to a mounting plate that is attached to the output of the rotary actuator. For ML aligned position adjustment, the linear actuator can move ±14*mm* along slots present in this mounting plate (Fig. 1 (a) and Fig. 3 (b)). A small end-effector assembly is attached at the end of the linear actuator spindle. The tip of the end-effector, which makes contact with the user's neck, is covered in silicon rubber to increase its coefficient of friction and to make it more comfortable to use. A load cell is housed inside the end-effector to continuously sense the interaction force. To reduce weight, majority of the components are made using 3D printed plastic. During use, the end-effector contacts the user's neck at the sternocleidomastoid muscle. This ensures that the pushing force delivered by it is always transferred to relatively thicker muscles and not to any delicate structures like blood vessels.

As shown in Fig. 2, the balance feedback system is divided into trunk and neck modules. This has been done to reduce the load imposed on the user's shoulders, which have to support the neck module. The neck module consists of the two NHDs, mounted one on each side of the user, and the required support structure described in section II C. The NHD can only generate skin indentation in the normal direction. Therefore, in order to provide feedback in both the medial and lateral

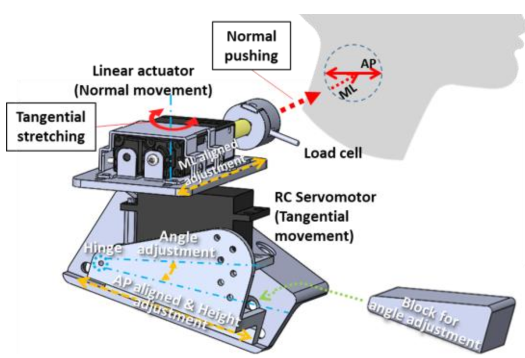

(a) Right side NHD

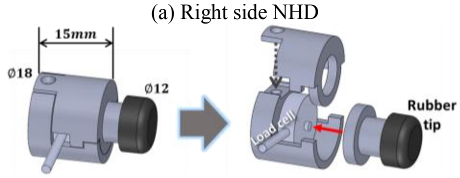

(b) NHD end-effector

Fig. 1. 3D models of the NHD.

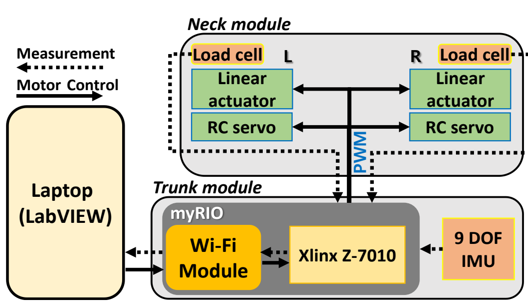

Fig. 2. Block diagram of the haptic feedback system.

TABLE I. DETAILS OF SYSTEM COMPONENTS

Component	Description
Linear actuator	Linear Servomotor, 12Lf-12PT-27, IR ROBOT®
Rotary actuator	RC Servomotor, DM-CLS119TD, DOMAN RC®
Load cell	CBMS, 30Kgf, 1mV/V, BONGSHIN®
Load cell amplifier	HX711, AVIA Semiconductor®
Attitude sensor	9DOF IMU, BNO055, Bosch®
Battery	Li-ion, DC12V/2.6Ah / 3.7V/2600mA*3ea, Coms®
Controller board	MyRIO 1900, National Instruments®

directions, two devices are required to provide indentations corresponding to each direction. In the presented system, the linear actuators work individually to provide skin indentation in their corresponding direction, whereas the rotary actuators both work together to generate the anterior and posterior directed skin stretches. However, due to system kinematics, the movement of each rotary actuator is influenced by the current position of the linear actuator attached to it. This is explained in the inverse kinematics part of section II B.

The trunk module, which is mounted on the waist belt described in section II C, includes the controller board (MCU) with onboard Wi-Fi module, the 9 axis inertial measurement unit (IMU), the load cell amplifiers, the power management hardware and the battery. The MCU reads the current trunk tilts at a rate of 100Hz from the IMU in the form of orientation quaternions, while the interaction force values are read from the load cell amplifiers. These data are transmitted to the PC over Wi-Fi. At the PC, a purpose-built software working in the LabVIEW (National Instruments, USA) environment processes the quaternion data using the method described in [23] to obtain the trunk tilt angles. These trunk tilt values are then processed using the methodology explained in the next section to generate the motor control values, which are transmitted to the MCU over Wi-Fi. The MCU converts the control values to PWM signals, which are sent to the motors where the motors' internal controllers ensure accomplishment of the desired movements. The trunk tilts, motor control values and force data are stored in the PC for later analysis. Details of system components are given in Table I.

B. Control Methodology

To allow skin stretching, the system has to be initially setup so that the end-effector is pressed 2-3*mm* into the skin. This position is considered as zero indentation position for ML directed feedback. Therefore, to deliver ML directed feedback, the linear actuator is moved beyond this initial position to further indent the skin. For ML directed feedback, when user tilts to the left, left side linear actuator is extended to cause skin indentation, and vice versa. For AP directed feedback,

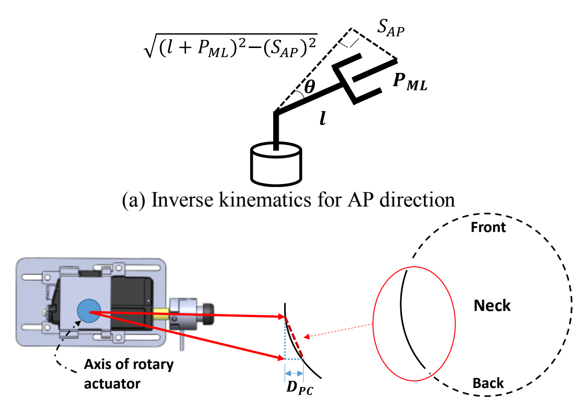

(a) Inverse kinematics for AP direction

(b) Pushing compensation (D_{PC}) for tilting in the forward direction

Fig. 3. Schematics for (a) inverse kinematics and (b) pushing compensation.

when user tilts forward, both rotary actuators move to stretch the skin on both sides of the neck towards the back side of the user, and vice versa. The equation for ML directed feedback (P_{ML}) is as follows.

$$P_{ML} = D_{Max.Pushing}\frac{TrunkTilt_{ML}}{Range_{ML}} \tag{1}$$

Here, $Range_{ML}$ is the maximum trunk tilt angle that the device should respond to, which was set to ±15 degrees in this study [24], $TrunkTilt_{ML}$ is the measured ML trunk tilt angle and $D_{Max.Pushing}$ is the maximum allowed displacement to give pushing feedback. Similarly, the relational equation for stretch in the AP direction (S_{AP}) is as follows.

$$S_{AP} = D_{Max.Stretch}\frac{TrunkTilt_{AP}}{Range_{AP}} \tag{2}$$

Here, $Range_{AP}$ is the maximum trunk tilt angle that the device should respond to, which is set as ±15 degrees [24], $TrunkTilt_{AP}$ is measured AP trunk tilt angle and $D_{Max.Stretch}$ is maximum tangential stretching displacement. Based on these relationships, skin indentation and stretching occur linearly by the ratio of current tilt angle with the maximum trunk tilt, which we refer to as the feedback ratio. The continuous feedback used here was selected based on the documented high efficacy of such type of haptic feedback for balance assistance [24-26], and the intuitive nature of continuous stimuli. Inverse kinematic equation for calculating actuation angle of the rotary actuator to generate required end-effector displacement determined using (2) is shown in (3).

$$\theta_{RCservo} = \arctan 2\left(\frac{S_{AP}}{\sqrt{(l+P_{ML})^2 - S_{AP}^2}}\right) \tag{3}$$

Here, l is distance from the central axis of rotary actuator to the end-effector tip when system is initially setup for operation, and P_{ML} is current linear actuator extension. System schematic used to derive this equation is shown in Fig. 3 (a).

As shown in Fig. 3 (b), when the device is moved to deliver skin stretching directed to the user's back, it is necessary to compensate for the curvature of the neck by extending the linear actuator so that the pushing feedback in ML direction is continuously maintained. In this study, this compensatory displacement, designated as D_{pc}, is set as 1*mm* based on our observations during preliminary tests that were carried out to tune the system's function. This compensatory movement is zero when the AP trunk tilt is zero or the user is tilting towards their backside (requiring forward directed stretching feedback). When user tilts to the front side (requiring backward directed stretching feedback) the compensatory movement increases linearly with AP trunk tilt

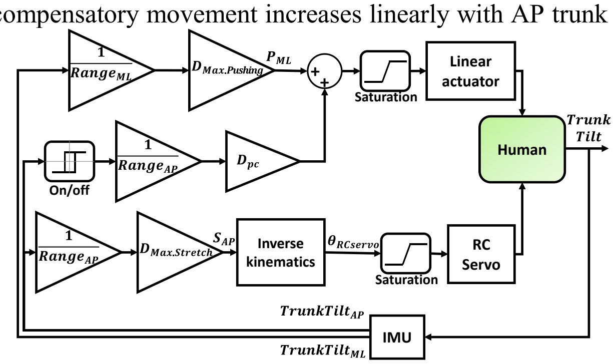

Fig. 4. Block diagram of the haptic feedback system.

TABLE II. SPECIFICATIONS OF THE DEVELOPED SYSTEM PROTOTYPE

Quantity	Specification		Requirement
	Normal	***Tangential***	
Force output	12N	10.24 ~ 18.63N	10N
Displacement	0 ~ 27*mm*	±90°	10*mm*
Adjustability	±14*mm*	±40*mm* (diagonal)	
Cue (10*mm*) Frequency	5.5Hz	37.88 ~ 67.57Hz	5Hz
Module	***Neck***		***Trunk***
Weight	890g (Devices 410g, Structure 480g)		570g

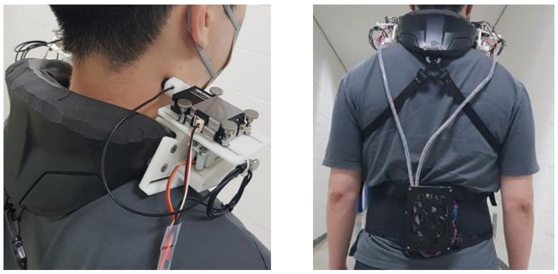

(a) Neck module (b) Trunk module

Fig. 5. The developed system prototype.

(a) T (b) O (c) G (d) R (e) W

Fig. 6. The experiment tasks. (a) Tandem Romberg stance (blindfolded), (b) One-leg stance (blindfolded) and (c) Tandem gait (eyes open) of healthy subjects. (d) Romberg stance (eyes open) and (e) Straight line walking (eyes open) of the stroke subject.

to reach the maximum value D_{pc} when the AP trunk tilt becomes equal to $Range_{AP}$, thus making the end-effector tip to follow the path shown by the red dashed line in Fig. 3 (b).

The system's operational block diagram is shown in Fig. 4. D_{Max} and *Range* values shown here are used to determine scale of movement. The device controller includes two safety features. First, saturation blocks included in the control loop ensure that the system does not move beyond the preset safe displacement limits. Second, if a force greater than the preset maximum level (10N was set in the experiments) is detected by the end-effector load cell, the linear actuator is rapidly moved (112mm/s) to the initial position, thus removing the force interaction. In order to avoid the complexity of hardware and calculations associated with gathering accurate 2D interaction force data between a device and the skin [18, 19], and due to the small magnitude of displacements occurring in the system, we have assumed the force data obtained from the load cell to be an acceptable representation of involved forces.

C. The System Prototype

The developed system prototype is shown in Fig. 5 while its specifications are given in Table II. A neck protector for motorcycle riders is repurposed as the structure for mounting the NHDs. This foam rubber structure sits on the user's shoulders and opens at the front to allow easy donning and doffing. Straps that pass under the user's armpits are attached to the structure for further stabilization. The trunk module is mounted on a waist belt with hook and loop fasteners that allow quick and easy donning and doffing while maintaining a snug fit that limits movement of the module with respect to the user's body. There is also a stiff foam insert placed under the electronics to stop the belt from sagging and to ensure user comfort. The waist-mounted part weighs 570g. It is expected that attaching this mass at the waist will have an added benefit of increasing the gait speed as it was shown that attachment of a similar mass to the waist of healthy and pathological subjects significantly increased gait speed [27].

Apart from the safety features mentioned in Section II B, three additional safety features have been included in the system to ensure the user's safeness. First, if the trunk tilt exceeds a preset value (15 degrees was set in the experiment), it is assumed that user is about to fall. In this case, both the actuators are rapidly moved (linear: 112mm/s, rotary: 857deg/s) to their zero positions. This takes the device hardware as far from the neck as possible, thus preventing any injury. Second, there is a software stop switch that the operator can press in case of an emergency. Lastly, a physical stop switch is fitted to the system that user can press if they do not want to continue using the system or in case of an emergency. When either of these switches is pressed, the system performs the same actions as it does when a fall is detected.

Prior to commencement of subject studies, we carried out bench tests to verify the feedback and safety functions of the developed system. To test the feedback, an experimenter moved the waist module to simulate individual and simultaneous movements in ML and AP directions. Tilts measured by the IMU and motor control commands during all tests were recorded and the results showed that the actuator commands very closely followed the trunk tilts. Furthermore, the commands became constant when tilts exceeded the maximum value, showing that the safety feature of limiting the skin deformation practically stops the actuator movements beyond the prescribed limit. The other safety features were tested by individually triggering each feature through button pressing, loading of the load cell and simulated falls. The tests proved that all the features work as intended (please see the accompanying video for details).

III. EXPERIMENTAL VALIDATION

A. Participants

An experiment was carried out to verify the functionality of the developed system prototype. 14 healthy people (7 male and 7 female) participated in this experiment (Age: 26.4± 6.5years, Height: 170.1±6.9*cm*, Weight: 64.0±12.1*kg*, dominant foot: Right 14). None of the participants suffered

TABLE III. PROTOCOL OF EXPERIMENTAL TRIALS

	Trial	Conditions
Healthy subject	TNN	**T**andem Romberg stance with **N**o device and **N**o feedback
	TDN	**T**andem Romberg stance with **D**evice and **N**o feedback
	TDF	**T**andem Romberg stance with **D**evice and **F**eedback
	ONN	**O**ne-leg stance with **N**o device and **N**o feedback
	ODN	**O**ne-leg stance with **D**evice and **N**o feedback
	ODF	**O**ne-leg stance with **D**evice and **F**eedback
	GNN	Tandem **G**ait with **N**o device and **N**o feedback
	GDN	Tandem **G**ait with **D**evice and **N**o feedback
	GDF	Tandem **G**ait with **D**evice and **F**eedback
Stroke subject	RNN	**R**omberg stance with **N**o device and **N**o feedback
	RDN	**R**omberg stance with **D**evice and **N**o feedback
	RDF	**R**omberg stance with **D**evice and **F**eedback
	WNN	Straight line **W**alking with **N**o device and **N**o feedback
	WDN	Straight line **W**alking with **D**evice and **N**o feedback
	WDF	Straight line **W**alking with **D**evice and **F**eedback

from any neurological, musculoskeletal or vestibular disorders. The study was approved by the Institutional Review Board at Gwangju Institute of Science and Technology, Gwangju, South Korea (20210609-HR-61-07-04). Furthermore, a pilot test was performed with 1 stroke patient at Gyeongsang National University Hospital (gender: male, age: 60years, height: 167cm, weight: 54.5kg, right-sided hemiplegia, 37 days since onset, cause of stroke: hemorrhage, Brunnstrom stages of stroke recovery: 4/4/4, modified Barthel index (MBI) score: 74, mini-mental state exam (MMSE) score: 21). All experiments were conducted in accordance with the Declaration of Helsinki. All subjects gave written informed consent before participation in the study.

B. Protocol

As shown in Fig. 6, the participants were asked to perform three tasks as part of the combined stance and gait balance test protocol [13, 24]. For stance balance evaluation with healthy subjects, the test included Tandem Romberg (T) and one-leg (O) stance conditions. Both these conditions were performed blindfolded and barefoot. In Tandem Romberg stance, the subject stood with the dominant foot placed in front of the non-dominant one in such a way that the toe of the rear foot touched the heel of the forward foot. In One-leg stance, the subject stood on their non-dominant foot with the dominant one raised up through flexion of the hip and knee of the dominant leg. Trial for each condition lasted 30 seconds and subjects were asked to keep their arms crossed across their chest under all test conditions. Foot dominance was established through the subject's preference in kicking a ball [11]. Before start of each stance trial, subjects were asked to stand in the prescribed pose and the system was calibrated to make their neutral posture equal to zero degrees of trunk tilt. During this calibration period, a researcher stabilized the subjects by lightly supporting them from both sides at upper arm level. This stabilizing support was removed when the test started. The gait task involved walking 5m barefoot with tandem gait (G) on a wooden beam (60 x 60 x 6200*mm*) [13, 28]. The subjects were asked to stand in their walking posture, one step behind the start line marked on the beam, and walk two steps beyond the finishing line (5*m*) marked on the beam. A gait speed measurement system (Seedtech, Korea) was used to measure the gait speed during the middle 5*m*. Other experimental conditions were same as the stance trials.

The stroke subject experiments were performed with eyes open and arms hanging naturally to ensure safety. For the stance condition, subject was asked to stand in the Romberg stance with feet as close together as possible and gaze at a flat wall to minimize visual effects in order to fully utilize the haptic feedback for balancing. A walker was placed in front of the subject for safety. For line walking, the subject was asked to walk along a straight line marked on the floor while placing their feet on or as close to it as possible. During all stroke subject trials, a doctor stood one step behind the subject and provided support before and after the trial. Other conditions were same as in the healthy subject experiments.

All the trial conditions consisting of three device and three feedback conditions are shown in Table III. In No device & No feedback (NN) condition, user does not wear the neck module of the device; however, they have to wear the waist module in order to measure the trunk sway. In Device & No feedback (DN) condition, user wears both the system modules in the initial setup condition (end-effectors pressed 2-3*mm* in to the skin), but the devices do not provide any feedback. In Device & Feedback (DF) condition, system is worn as described in the previous condition and trunk tilt feedback is provided in the form of skin deformation. Feedback ratios were selected based on our observations during preliminary tests. During the stance balance evaluation trials, due to the relatively smaller magnitudes of trunk tilts, the feedback in both directions is given in a 1:3 ratio of $Range_{tilt}$:D_{Max}. The minimum perceivable deformation of the skin at the neck is 1.5*mm* [20], therefore this feedback ratio was selected so that the subject can sense the feedback produced with the minimum tilt of 0.5 degree. With this relationship, if the body tilts 0.5 degree, 1.5mm feedback is given. For the gait trials, due to the relatively larger magnitude of trunk tilts, the feedback ratio for both directions was set as 1:2 so that the maximum motion limits of the NHDs are not reached too often during the trials. According to these ratios, for the maximum tilt limit ($Range_{tilt}$) of ±15 degrees in both the ML and AP directions, the maximum displacement values (D_{Max}) of 30*mm* and 45*mm* were used for the 1:2 and 1:3 feedback ratios, respectively. For example, 1:3 means 3*mm* feedback is generated for 1 degree trunk tilt. Two trials were performed under each condition and all the conditions were performed in pseudo-random order to avoid any sequence related effects.

C. Data Analysis

Trunk tilt data from the on-board sensor and operational data of the feedback devices were recorded during all trials. Data from the middle 25 seconds of the stance trials and 25 seconds of data recorded after the first 2.5 seconds of the gait trials were used for analysis. From the ML and AP trunk tilt angles recorded during the trials, projections of trunk tilt (PT) were calculated using (4) and (5):

$$PT_{ML} = TrunkTilt_{ML} \times h \tag{4}$$

$$PT_{AP} = TrunkTilt_{AP} \times h \tag{5}$$

Where, h is IMU sensor mounting height from the ground and $TrunkTilt_{ML}$ and $TrunkTilt_{AP}$ are trunk tilts in ML and AP directions, respectively. The calculated *PT* values were used to calculate mean velocity displacement (*MVD*), planar deviation (*PD*), ML trajectory (*MLT*) and AP trajectory (*APT*), which are commonly used indices for evaluating body sway [24]. These indices are calculated using following equations:

$$MVD(cm/s) = \frac{\sum_{i=1}^{n} \frac{\sqrt{((PT_{ML}(i) - PT_{ML}(i-1))^2 + (PT_{AP}(i) - PT_{AP}(i-1))^2)}}{t_i - t_{i-1}}}{n} \tag{6}$$

$$PD(cm) = \sqrt{\sigma^2 PT_{ML} + \sigma^2 PT_{AP}} \tag{7}$$

$$MLT(cm) = \sum \left| PT_{ML}(i+1) - PT_{ML}(i) \right| \tag{8}$$

$$APT(cm) = \sum \left| PT_{AP}(i+1) - PT_{AP}(i) \right| \tag{9}$$

MVD is the combined mean value of ML and AP *PT* velocities that shows overall rate of *PT* displacement. Square root of sum of variances (σ^2) of *PT* displacements in both the ML and AP directions yields the *PD* value, which shows the spread of the *PT*. *MLT* and *APT* are respectively the sums of changes in the ML and AP *PT* values, which shows the overall amount of *PT* displacement. For all these indices ((6)–(9)), larger values indicate greater levels of balance difficulty [24].

A 2-way RMANOVA was used to investigate the effects of Device & Feedback (NN, DN, DF) and Task (T, O, G) on MVD, PD, MLT and APT of healthy subjects. Furthermore, 1-way RMANOVA was used to analyze differences in gait speed between gait trials of healthy subjects. Mauchly's test of Sphericity was used to check validity of RMANOVA results ($p < .05$) and Greenhouse Geisser corrections (for $\varepsilon < .75$) were applied in case of its violation. Post hoc tests were conducted with application of Bonferroni correction. Partial eta squared (η_p^2) was calculated as a measure of the effect size for 1- and 2-way RMANOVA. All statistical analyses were conducted using SPSS V20.0 (IBM Corp., USA).

IV. Results

PT Stabilograms of one healthy and stroke subject under all trial conditions are shown in Fig. 7. It is apparent that feedback delivered by the developed system, for the most part, reduces the spread of subject's trunk tilts. A more congested stabilogram indicates greater balance control [29].

Feedback delivered under different trial conditions was recorded. Under all conditions the system displacements remained well within the operational limit of 20*mm* (Healthy:13.5±4.5*mm*, Stroke: 9.1±1.8*mm*). Furthermore, force data from load cells embedded in the end-effectors showed that a maximum force of 4.97N (left side, during healthy gait trial) was applied by the system, which is far below the designed force limit of 10N. The mean force during the same trial was 1.4±0.8 N (left side, all healthy subjects).

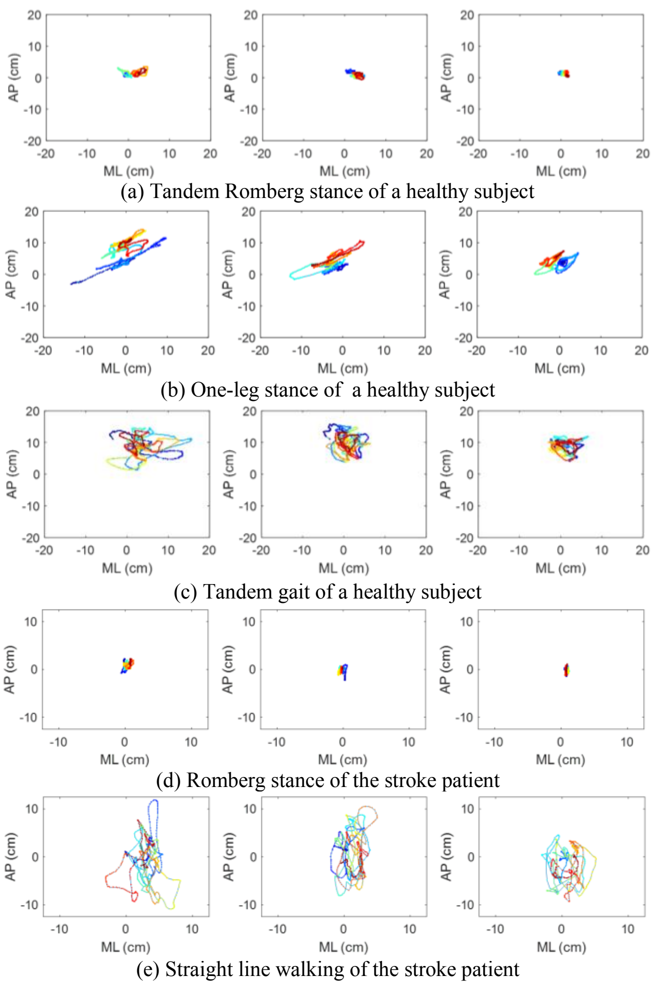

Fig. 7. The stabilograms (*PT*) of a healthy and a stroke subject during all trials. In each figure, first column is NN, second column is DN and third column is DF device condition. Red to blue color transition represents trial time from start to end.

The gait speed results are presented in Fig. 8. A 1-way RMANOVA revealed no significant differences in gait speed of healthy subjects between GNN, GDN and GDF conditions ($F(2, 26) = .213$, $p < .810$, $\eta_p^2 = .016$). These results show that use of the developed system does not have a detrimental effect on the subject's gait. The effects of using this system on the participants' gait balance are discussed in the following section. Similar to healthy subjects' results, speed results of the stroke subject pilot test (W trial) also did not show any substantial variation. However, the speed was higher than that of the healthy subjects, which is attributed to walking on a line instead of the beam. Standard deviation values shown in Fig. 8 and 9 are computed across subjects for the healthy subjects and across trials for the stroke subject.

Results of 2-way RMANOVA are presented in Table IV. No significant interaction of Task (One-leg stance, Tandem Romberg stance and Gait) and Device (NN, DN and DF) led to main effect analysis and post-hoc pairwise comparisons of Task and Device separately for all measures. Main effects for all tasks show highly significant differences ($p < .001$). This means that the tasks differ appropriately in terms of difficulty. Results of 1-way RMANOVA performed for each task are presented in Fig. 9 (a), (b), (c) and (d). Due to use of different feedback ratios in stance and gait trials, results of main effects tests for Device condition are omitted. It can be observed that none of the indices show any significant difference between NN and DN conditions. This shows that just wearing the device under the condition that initial force is applied to the neck to allow delivery of skin stretch feedback does not have any significant detrimental effect on the subjects' balance.

V. Discussion

The presented system was developed to gain the benefit of freeing up the user's hands while preserving the effects of haptic balance biofeedback during standing and walking. As mentioned earlier, some systems have been developed for this purpose but they do not deliver haptic cues in the form of hybrid skin deformation of the neck [10-13]. Unlike those devices, our system has the ability to provide two dimensional directed feedback. Furthermore, the reaction wheel system that we had previously developed, suffered from low force output that was not perceivable due to high inertia of the body during gait [11, 12]. This limitation can be overcome by using gyroscopic actuators [13], but due to the mass of the flywheel and structural components required to ensure user safety, such a system becomes relatively large and heavy. In the presented system, mounting of actuators on the user's shoulders allows

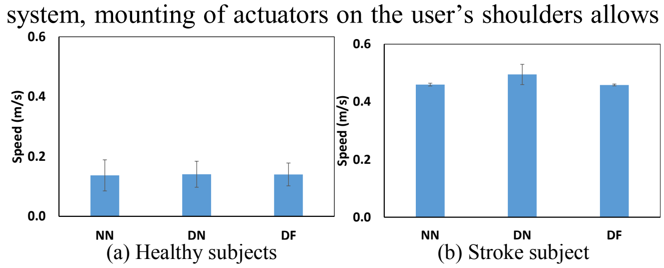

Fig. 8. The gait speed results of (a) healthy subjects and (b) the stroke subject. Error bars show the standard deviation. No device and No feedback (NN), Device and No feedback (DN), Device and Feedback (DF).

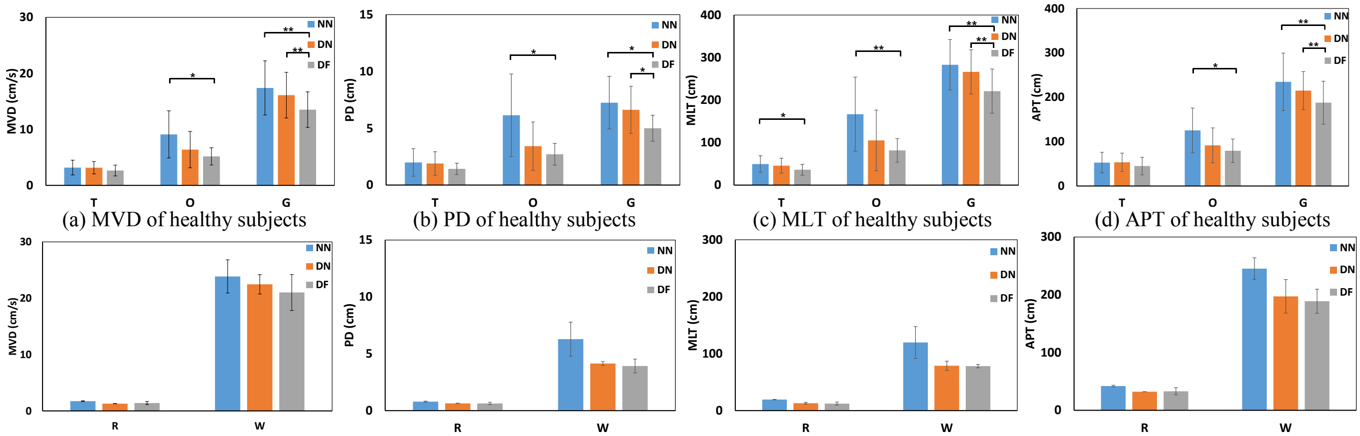

(a) MVD of healthy subjects (b) PD of healthy subjects (c) MLT of healthy subjects (d) APT of healthy subjects

(e) MVD of the stroke subject (f) PD of the stroke subject (g) MLT of the stroke subject (h) APT of the stroke subject

Fig. 9. Results of 1-way RMANOVA of healthy subject experiments, and stroke subject experiment. Statistically significant differences are marked based on Post-hoc pairwise comparisons (*: p<0.05, **: p<0.01, *** p<0.001). Error bars show the standard deviation. Tandem Romberg stance (T), One-leg stance (O), Tandem gait (G), Romberg stance (R), Straight line walking (W), No device and No feedback (NN), Device and No feedback (DN), Device and Feedback (DF).

us to generate the desired stimuli without requiring large and heavy actuators and structures, thus making it considerably lighter and more compact than the other systems.

Results show that compared to NN condition, velocity and trajectory of 2-dimensional body sway were significantly reduced under DF condition (See Fig. 9 (a), (b), (c) and (d)). It means that the developed system can reduce the velocity and range of displacement, and total amount of movement in both the ML and AP directions simultaneously. Interestingly, results also show that more difficult the task, more significant the effect of the developed system. As compared to the O task condition (NN vs. DF: MVD, PD, APT; $p < .05$, MLT; $p < 0.01$), delivery of balance feedback during the G task condition resulted in more significant reductions in MVD, PD, MLT and APT (NN vs. DF: MVD, MLT, APT; $p < .01$, PD; $p < 0.05$ and DN vs. DF: MVD, MLT, APT; $p < .01$, PD; $p < 0.05$) (Fig. 9 (a), (b), (c) and (d)). Therefore, it is expected that the developed feedback strategy may have higher efficacy under more dynamic conditions such as walking. Furthermore, there was no significant difference in walking speed in the tandem walking condition. This indicates that the system does not impose a high cognitive load on the user, which can result in reduced gait speed [30]. Therefore, the proposed system may improve the user's balancing ability through sensory augmentation without putting a high cognitive load on them, thus making it suitable for use by elderly persons or patients who have diminished cognitive ability.

Tandem-Romberg stance causes disturbance mainly in the ML direction. Under this condition, feedback delivered by the system did not have any significant effect on the experimental outcomes, apart from the MLT. Therefore, it can be inferred that application of the feedback helps to reduce the total amount of ML movement under this condition, but does not have a significant effect on the velocity and range of displacement. There are two possible reasons for this outcome. First, values of the outcome measures under this condition are relatively small, which indicates that body movements in this stance were of a very small order. Such small movements result in only a small amount of feedback, which perhaps was not enough to elicit a response from the participants. Furthermore, feedback below the perceptible threshold can cause the origin position to be lost. An increase in the feedback ratio may solve this issue but it will limit the maximum trunk tilt for which the system can provide feedback. Therefore, a dead zone surrounded by an abrupt (binary) feedback that then changes proportionally with the tilt may solve these issues. Another issue is that if the tilt is happening slowly, the change in feedback also occurs at a slow pace. This can result in the feedback going unnoticed by the user due to sensory adaptation of the skin [31]. This may be overcome if instead of a constant deformation, the feedback is provided in the form of repeated skin deformations. These solutions and other feedback strategies will be tested in the future to find the best performing strategy.

As shown in Fig. 9 (a), (b), (c) and (d), during the O trials, the mean values of all measures under the DN condition were lower than those under the NN condition. Whereas, there was no significant difference in any of the values between the DN and DF conditions. This is an interesting observation, which indicates that even the application of a small amount of constant pushing on the neck that is not modulated according to the trunk tilt, may improve a person's balance. However, the large standard deviations of the outcome measures under these conditions indicate that the prevalence of this effect may vary from person to person. On the other hand, during the G trials, there were significant differences in all the measures between DN and DF conditions. These results show that in stance conditions, simply pressing on the neck may have an effect on the balance, which may not be significantly enhanced through modulation of the force according to the user's balance. However, such a limitation may not be present under the dynamic gait condition. The verification and further explorations of this effect will be carried out in the future.

Pilot testing with a stroke subject produced results that were similar to the healthy subjects. Wearing the device in no

TABLE IV. RESULTS OF THE 2-WAY RMANOVA

Parameter	Factor	F	P-value	η_p^2
MVD (cm/s)	Task	(1.35, 17.58) = 91.27	**< .001**	**.875**
	Device	(2, 26) = 23.14	**< .001**	**.640**
	Interaction	(2.12, 27.50) = 2.88	.071	.181
PD (cm)	Task	(2, 26) = 53.54	**< .001**	**.805**
	Device	(2, 26) = 13.62	**< .001**	**.512**
	Interaction	(2.10, 27.34) = 2.80	.076	.177
MLT (cm)	Task	(2, 26) = 124.05	**< .001**	**.905**
	Device	(1.41, 18.29) = 21.83	**< .001**	**.627**
	Interaction	(2.06, 26.82) = 3.04	.063	.189
APT (cm)	Task	(1.37, 17.80) = 138.09	**< .001**	**.914**
	Device	(1.42, 18.52) = 20.64	**< .001**	**.614**
	Interaction	(1.99, 25.89) = 2.83	.078	.179

feedback condition improved balance, showing that stroke subjects' balance may also be sensitive to force contact at the neck. The balance improvements with feedback show that the developed feedback system may be a feasible method for balance rehabilitation of stroke survivors. Furthermore, the subject was comfortable with using this system and expressed their confidence in it. These promising results pave the way for further studies to determine the efficacy of this system and its feedback in improving balance of stroke survivors.

VI. Conclusion

This work proposed a wearable balance biofeedback system that delivers 2-dimensional hybrid haptic biofeedback to the neck that is a combination of indentation and stretching of the skin. The system's functionality is demonstrated through experiments where 14 healthy subjects and 1 stroke subject performed stance and gait tasks under various conditions. Results show that the feedback delivered by the proposed system has an improving effect on the user's balance under both stance and gait conditions. The effects observed with the current system, which uses skin deformation as the feedback modality, show the same trends as those observed with a light-touch force interface [17]. This indicates that use of skin deformation as a feedback modality is a viable choice for the design of a simple and cost-effective feedback system. However, some limitations on the effectiveness of the feedback strategy in relation to the slow trunk movements were observed during this study. It is expected that these limitations can be overcome through the development of more elaborate feedback strategies, which will enable us to gain the most benefit from the use of this system for balance rehabilitation, especially during overground gait.

References

[1] V. L. Feigin *et al.*, "Global and regional burden of stroke during 1990-2010: findings from the Global Burden of Disease Study 2010," *Lancet*, vol. 383, no. 9913, pp. 245–254, 2014.

[2] P. A. Goldie, T. A. Matyas, O. M. Evans, M. Galea, and T. M. Bach, "Maximum voluntary weight-bearing by the affected and unaffected legs in standing following stroke," *Clin. Biomech. (Bristol, Avon)*, vol. 11, no. 6, pp. 333–342, 1996.

[3] Y. Jung, K. Lee, S. Shin, and W. Lee, "Effects of a multifactorial fall prevention program on balance, gait, and fear of falling in post-stroke inpatients," *J. Phys. Ther. Sci.*, vol. 27, no. 6, pp. 1865–1868, 2015.

[4] M. V. Radomski and C. A. T. Latham, "Occupational therapy for physical dysfunction." Lippincott Williams & Wilkins, 2008.

[5] E. R. Walker, A. S. Hyngstrom, and B. D. Schmit, "Influence of visual feedback on dynamic balance control in chronic stroke survivors," *J. Biomech.*, vol. 49, no. 5, pp. 698–703, 2016.

[6] K. Gordt, T. Gerhardy, B. Najafi, and M. Schwenk, "Effects of wearable sensor-based balance and gait training on balance, gait, and functional performance in healthy and patient populations: A systematic review and meta-analysis of randomized controlled trials," *Gerontology*, vol. 64, no. 1, pp. 74–89, 2018.

[7] E. Swinnen, D. Beckwée, R. Meeusen, J.-P. Baeyens, and E. Kerckhofs, "Does robot-assisted gait rehabilitation improve balance in stroke patients? A systematic review," *Top. Stroke Rehabil.*, vol. 21, no. 2, pp. 87–100, 2014.

[8] A. R. Oates, L. Hauck, R. Moraes, and K. M. Sibley, "The effects of haptic input on biomechanical and neurophysiological parameters of walking: A scoping review," *Gait Posture*, vol. 58, pp. 232–239, 2017.

[9] S.-H. Pyo, M.-G. Oh, and J.-W. Yoon, "Development of an active haptic cane for gait rehabilitation," in *Proc. 2015 IEEE Int. Conf. on Robotics and Automation*, Seattle, 2015, pp. 4464-4469.

[10] B.-C. Lee, A. Fung, and T. A. Thrasher, "The effects of coding schemes on vibrotactile biofeedback for dynamic balance training in Parkinson's disease and healthy elderly individuals," *IEEE Trans. Neural Syst. Rehabil. Eng.*, vol. 26, no. 1, pp. 153–160, 2018.

[11] M. R. Afzal, A. Eizad, C. E. Palo Peña, and J. Yoon, "Evaluating the effects of kinesthetic biofeedback delivered using reaction wheels on standing balance," *J. Healthc. Eng.*, vol. 2018, pp. 1–10, 2018.

[12] A. Eizad, M. R. Afzal, H. Lee, J. Yoon, and S.-K. Lyu, "A wearable reaction wheel based kinesthetic biofeedback device for delivery of balance cues," in Proc. *19th Int. Conf. on Control, Automation and Systems*, Jeju, 2019, pp. 173-178.

[13] D. Lemus *et al.*, "Controller synthesis and clinical exploration of wearable gyroscopic actuators to support human balance," *Sci. Rep.*, vol. 10, no. 1, p. 10412, 2020.

[14] I. Hussain, G. Spagnoletti, C. Pacchierotti, and D. Prattichizzo, "A wearable haptic ring for the control of extra robotic fingers," in *Lecture Notes in Electrical Engineering*, Singapore: Springer Singapore, 2018, pp. 323–325.

[15] F. Chinello, C. Pacchierotti, M. Malvezzi, and D. Prattichizzo, "A novel 3RRS wearable fingertip cutaneous device for virtual interaction," in *Lecture Notes in Electrical Engineering*, Singapore: Springer Singapore, 2018, pp. 63–65.

[16] F. Chinello, C. Pacchierotti, N. G. Tsagarakis, and D. Prattichizzo, "Design of a wearable skin stretch cutaneous device for the upper limb," in Proc. *IEEE Haptics Symposium*, Philadelphia, 2016, pp. 14-20.

[17] V. Krishnamoorthy, H. Slijper, and M. L. Latash, "Effects of different types of light touch on postural sway," *Exp. Brain Res.*, vol. 147, no. 1, pp. 71–79, 2002.

[18] H. Joodaki and M. B. Panzer, "Skin mechanical properties and modeling: A review," *Proc. Inst. Mech. Eng. H*, vol. 232, no. 4, pp. 323–343, 2018.

[19] L. Zou, C. Ge, Z. Wang, E. Cretu, and X. Li, "Novel tactile sensor technology and smart tactile sensing systems: A review," *Sensors (Basel)*, vol. 17, no. 11, p. 2653, 2017.

[20] J. Biggs and M. A. Srinivasan, "Tangential versus normal displacements of skin: relative effectiveness for producing tactile sensations," in Proc. *10th Symp. on Haptic Interfaces for Virtual Environment and Teleoperator Systems*, Orlando,2002, pp. 121-128.

[21] V. P. Panzer, S. Bandinelli, and M. Hallett, "Biomechanical assessment of quiet standing and changes associated with aging," *Arch. Phys. Med. Rehabil.*, vol. 76, no. 2, pp. 151–157, 1995.

[22] T. Ji, and A. Pachi, "Frequency and velocity of people walking." *The Structural Engineer*, vol. 84, no. 3, pp. 36-40, 2005.

[23] H. Lee, A. Eizad, Y. Kim, Y. Park, M.-K. Oh, and J. Yoon, "Use of vibrotactile bracelets to study effects of arm swing variation on overground gait," *IEEE Access*, vol. 9, pp. 90896–90907, 2021.

[24] M. R. Afzal, H.-Y. Byun, M.-K. Oh, and J. Yoon, "Effects of kinesthetic haptic feedback on standing stability of young healthy subjects and stroke patients," *J. Neuroeng. Rehabil.*, vol. 12, no. 1, p. 27, 2015.

[25] Shull PB, Damian DD. Haptic wearables as sensory replacement, sensory augmentation and trainer–a review. Journal of neuroengineering and rehabilitation. 2015 Dec;12(1):1-3.

[26] Sienko KH, Balkwill MD, Oddsson LI, Wall C. The effect of vibrotactile feedback on postural sway during locomotor activities. Journal of neuroengineering and rehabilitation. 2013 Dec;10(1):1-6.

[27] H. S. Yang *et al.*, "'Effects of arm weight on gait performance in healthy subjects,'" *Hum. Movement Sci*, vol. 60, pp. 40–47, 2018.

[28] A. A. da S. Costa, L. O. dos Santos, E. Mauerberg-deCastro, and R. Moraes, "Task difficulty has no effect on haptic anchoring during tandem walking in young and older adults," *Neurosci. Lett.*, vol. 666, pp. 133–138, 2018.

[29] T. E. Prieto, J. B. Myklebust, R. G. Hoffmann, E. G. Lovett, and B. M. Myklebust, "Measures of postural steadiness: differences between healthy young and elderly adults," *IEEE Trans. Biomed. Eng.*, vol. 43, no. 9, pp. 956–966, 1996.

[30] A. W. Priest, K. B. Salamon, and J. H. Hollman, "Age-related differences in dual task walking: a cross sectional study," *J. Neuroeng. Rehabil.*, vol. 5, no. 1, p. 29, 2008.

[31] Q. Wang, R. M. Webber, and G. B. Stanley, "Thalamic synchrony and the adaptive gating of information flow to cortex," *Nat. Neurosci.*, vol. 13, no. 12, pp. 1534–1541, 2010.